NEES/E-Defense Base Isolation Tests: Performance of Triple-Pendulum Bearings

T. Okazaki, K. Sato
Hokkaido University, Japan

E. Sato, T. Sasaki & K. Kajiwara
National Research Institute for Earth Science and Disaster Prevention, Japan

K. Ryan
University of Nevada, Reno, U.S.A.

S. Mahin
University of California, Berkeley, U.S.A.

SUMMARY:
This is one of four papers reporting a NEES/E-Defense collaborative program on base-isolated buildings. A full-scale, five-story, two-by-two bay, steel moment-frame building was subjected to a number of bidirectional and bidirectional-plus-vertical ground motions using the E-Defense shake table. The building was tested under three different configurations: 1) base isolated with triple-friction-pendulum bearings (TPBs), 2) base isolated with a combination of lead-rubber bearings (LRBs) and cross-linear bearings (CLBs), and 3) base fixed. This paper describes the response of individual TPBs used in configuration (1). The aspect ratio of the building was 0.82 and 0.68, respectively, in the two floor-plan directions. The large overturning moment in the building combined with the vertical shake-table motion produced substantial variation in the vertical forces in the TPBs. Some of the larger motions caused uplift (disengagement of components) in the TPBs. The measured response of TPBs is discussed with emphasis on the effect of varying vertical loads.

Keywords: Seismic isolation; Shake-table test; triple-friction-pendulum bearings; force versus displacement relationship; uplift.

1. INTRODUCTION

This is one of four papers reporting a collaborative research program on base-isolated buildings conducted under the Memorandum of Understanding between the National Institute of Earth Science and Disaster Prevention (NIED) of Japan and the National Science Foundation (NSF), George Brown Jr. Network for Earthquake Engineering Simulation (NEES) program of the U.S. A full-scale, five-story, two bay-by-two bay, steel moment-frame building was subjected to a number of bidirectional (XY) and bidirectional-plus-vertical (XYZ) ground motions using the NIED E-Defense shake table. The building was tested under three different configurations: 1) base isolated with triple-friction-pendulum bearings (TPBs), 2) base isolated with a combination of lead-rubber bearings (LRBs) and cross-linear bearings (CLBs), and 3) base fixed. Nonstructural components and loose contents were installed on the fourth and fifth floors of the building. An overview of the test program and a comparison of the structural response in the three configurations are reported by Sasaki et al. (2012). The influence of vertical excitation on the response of the base-isolation systems is reported by Ryan et al. (2012). The behavior of nonstructural components is reported by Soroushian et al. (2012).

This paper describes the response of individual triple-friction-pendulum bearings (i.e., the TPBs in configuration (1). Overturning moment in the superstructure combined with vertical shake-table motion produced substantial variation in the compression in the TPBs. In fact, some of the larger motions caused uplift (disengagement of components) in some of the TPBs. Consequently, the test produced a rich set of data on full-scale TPBs subjected to a range of interesting dynamic loading conditions. The remainder of the paper describes selected aspects of the test plan, describes the measured response of TPBs, and examines the effect of varying compression on the measured response.

2. TEST PLAN

2.1. Specimen Configuration

Fig. 1 shows the North elevation and a typical floor plan of the steel building, along with the orientation and Cartesian coordinate system used throughout this paper. The two bay-by-two bay, five story building was 10 m and 12 m wide, respectively, in the X and Y-directions, and 15.8 m tall. The total mass of the building was 543 metric tons including a 54-ton mass on the roof that introduced a 10% eccentricity (distance between center of mass and center of rigidity divided by the floor plan dimension) in the roof in the EW-direction and a rigid base comprising 900-mm-deep beams. Fig. 2 shows the vertical distribution of mass. The aspect ratio of the building, taken as the height of mass center divided by the floor plan dimension, was 0.82 and 0.68 in the X and Y-directions, respectively. From white noise excitation tests under the base-fixed configuration, the fundamental vibration frequency of the superstructure was determined as 0.7 s in both X and Y-directions. Further details of the building specimen are provided by Sasaki et al. (2012).

Fig. 3 shows the location of base-isolation bearings in the TPB system. The figure also indicates the edges of the shake table and the building envelope. The TPB system placed nine TPBs, one below each of the nine columns. The bearings are identified according to their relative locations, for example, as S for South edge, C for center, and NE for North-East corner. Table 1 lists the gravity load measured at each bearing prior to testing. The measured load was between 430 and 850 kN and was somewhat different from the load estimated from tributary floor areas. Bearings SE, SW, C, and W were subjected to only half the load placed on Bearing E. It proved to be an extreme challenge to place

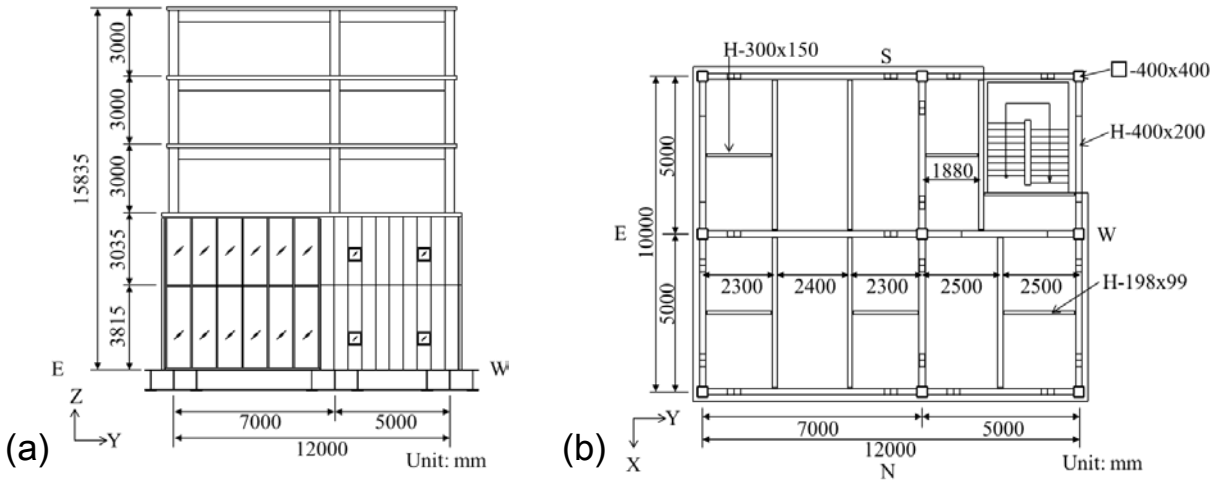

Figure 1. Outline of the building: (a) North elevation; and (b) typical floor plan. (Dimensions in mm).

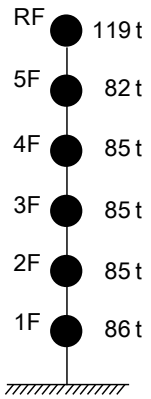

Figure 2. Mass distribution

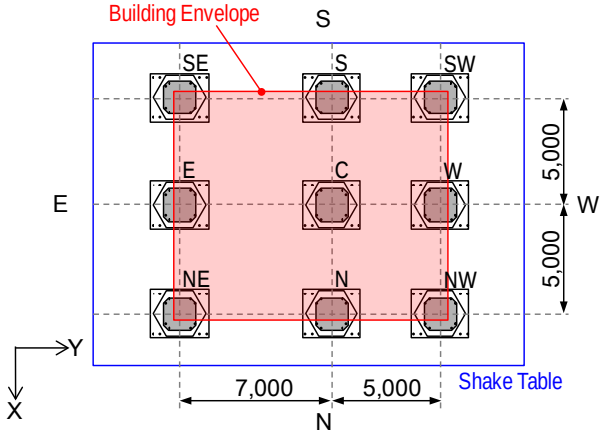

Figure 3. Location of TBS. (Dimensions in mm).

Table 1. Initial vertical loads (in kN)

SE 437	**S** 786	**SW** 442
E 848	**C** 484	**W** 478
NE 642	**N** 600	**NW** 529

a constructed superstructure evenly on nine bearings. It is also recognized that overturning moments should cause more substantial variation in compression in the corner bearings. Therefore, intuition suggests that Bearings SE and SW were most likely to experience uplift (vertical disengagement of components) during severe motions, while Bearing E was much less likely to experience uplift.

2.2. Instrumentation

Six displacement transducers were placed as indicated in Fig. 4 to measure the relative motion between the base beams and shake table. The geometric relationship between the translation and rotation of the rigid base and change in the measured distances was used to compute the bidirectional displacement at each bearing.

An assembly of seven to nine tri-directional load cells was placed under each bearing to measure three-directional force components. Fig. 5 shows how nine load cells were placed underneath Bearing C in combination with two, 100-mm steel plates. Accelerometers were placed on the upper steel plate. The force components were evaluated at level A-A' indicated in the figure by subtracting the horizontal inertia and weight of the plate from the load cell measurements. Fig. 6 compares the X and Y shear forces at the isolation layer measured from two different instrumentation systems. One is the sum of load cell measurements from all nine bearings, and the other is the sum of inertia produced at all floors, where the inertia is obtained as the product of the mass shown in Fig. 2 and measured floor acceleration. The figure shows the time history obtained from the 100%-XYZ Takatori motion. The

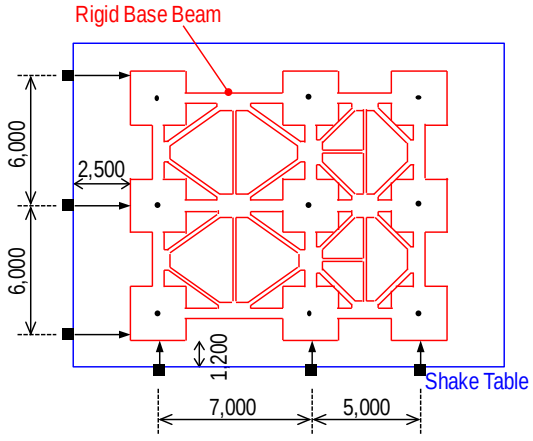

Figure 4. Displacement transducers (Dimensions in mm).

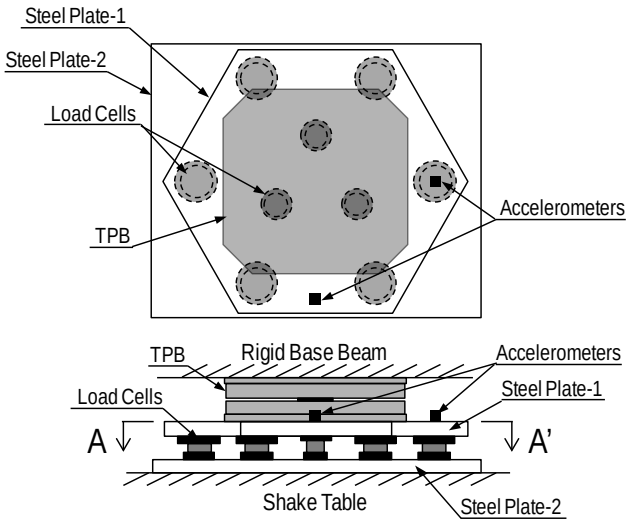

Figure 5. Load cells at Bearing C

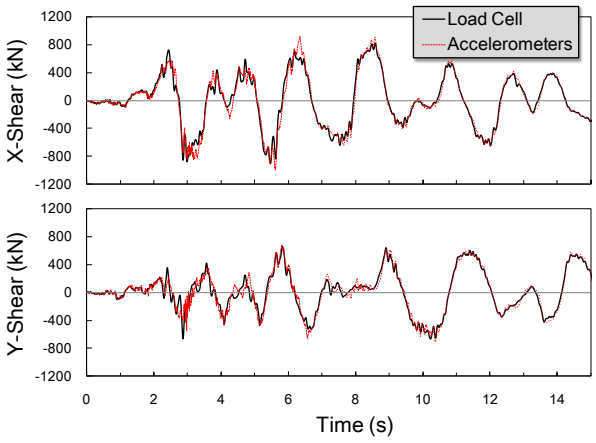

Figure 6. Shear in isolation layer evaluated from independent instrumentation systems

very good match between the two instrumentation systems suggests that the load cell measurements were quite reliable.

2.3. TPB Bearings

As described by Fenz and Constantinou (2008) and Morgan and Mahin (2011), the hysteretic response of TPBs is controlled by the dimensions and friction coefficient of the spherical sliding surfaces. The horizontal reaction is proportional to the vertical force. Fig. 7 shows the target hysteresis of the TPBs used in the tests plotting the normalized horizontal force F_x/F_z against a unidirectional displacement u. The parameters were chosen so that the TPBs act in two stages rather than in three stages. The TPBs were designed to act rigidly (stage 0) until the friction coefficient 0.02 of the inner pendulum is overcome. The inner pendulum is activated (stage 1) until the friction coefficient 0.08 of the outer pendulum is overcome, beyond which the outer pendulum is activated (stage 2). When the displacement limit of the outer pendulum 1.08 m is exceeded, the inner pendulum is once again activated (stage 3). At a displacement of 1.13 m, both the inner and outer pendulums bear against their respective circular rim. Upon load reversal, the response stages are activated in the same order as stage 0, 1, 2, and finally 3. The response period is evaluated as 1.84 sec for stages 1 and 3, and 5.57 sec for stage 2. A key benefit that distinguishes TPBs from other base-isolation devices is that the response period is independent of the applied weight (vertical force). Consequently, TPBs are suitable for use in light structures, extremely heavy structures, and structures with substantial mass eccentricity.

2.4. Loading Program

The TPB system was subjected to a total of twenty-one motions. This paper will primarily discuss the response obtained from (a) sinusoidal motion, (b) the Rinaldi Receiving Station motion from the 1994 Northridge earthquake, reproduced in 88%-scale in XY and XYZ, (c) the JR Takatori Station motion from the 1995 Kobe earthquake, reproduced in 100% in XYZ, (d) the K-NET Iwanuma motion from the 2011 Tohoku earthquake, reproduced in 100% in XY, and (e) the Tabas Station motion from 1978 Tabas earthquake, reproduced in 80% in XYZ and in 100% in XY. Fig. 8 shows the acceleration response spectra for the NS and EW components of the original motions (target for 100% motion) for a damping ratio of 0.05. The solid and dotted lines show the response spectra for the NS and EW

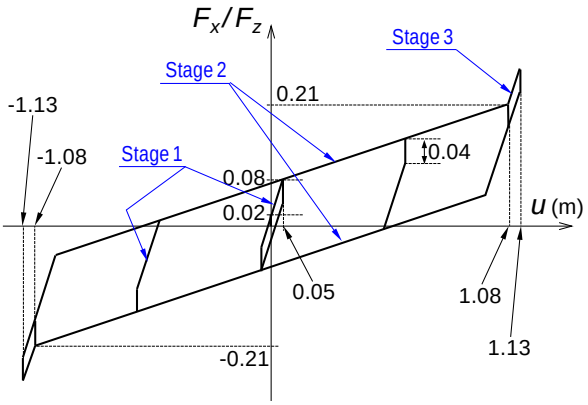

Figure 7. Target force-displacement relationship

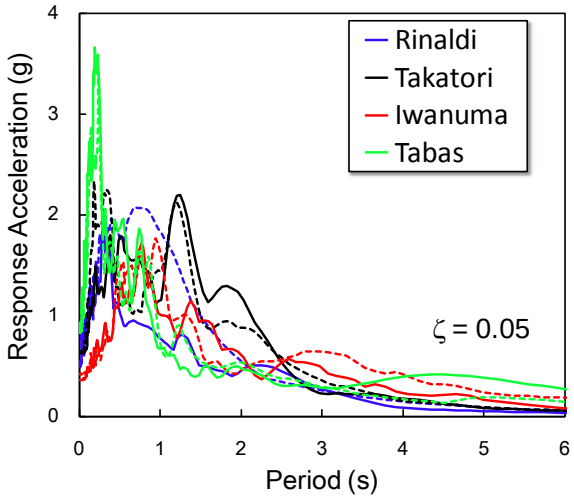

Figure 8. Acceleration Response Spectra

Table 2. Peak ground acceleration (in g)

	Rinaldi	Takatori	Iwanuma	Tabas
NS	0.49	0.75	0.36	0.85
EW	0.83	0.62	0.42	0.84
UD	0.83	0.29	(0.25)	0.69

components, respectively. The response spectra indicate that all motions are very demanding over a wide period range. In particular, the Takatori motion is extremely demanding in the period range of 1 to 2 seconds. The Iwanuma and Tabas motions have substantial long period contents. Table 2 lists the peak ground accelerations for each motion. It is noted that the UD components of the Rinaldi and Tabas motions are very large.

3. TEST RESULTS

3.1. Characterization Tests

Fig. 9 shows the hysteresis of all nine bearings obtained from a unidirectional motion that produced a sinusoidal response in the X-direction. The figure takes the horizontal displacement u_x as the abscissa and the horizontal force F_x normalized by vertical force F_z as the ordinate. The inclined dotted lines indicate the target response when the outer pendulums are activated (stage 2 in Fig. 7) assuming a friction coefficient of 0.08. All bearings responded similarly and overall, the measured response agreed quite well with the target hysteresis in Fig. 7. However, the friction coefficients tended to be larger than the targeted 0.08. To be more specific, substantially larger friction coefficients were observed in Bearings N and NE in the negative F_x side and in Bearing SE, S, and SW in the positive F_x side. The large friction coefficient was observed at instances when the vertical force F_z was reduced due to overturning moment in the superstructure. Between three south-side bearings SE, S, and SW, SE and SW, which were subjected to smaller gravity load (442 and 437 KN, respectively, as listed in Table 1) saw a larger increase in friction coefficient than S, which was subjected to twice the gravity load (786 kN). Bearing E, which was subjected to the largest gravity load among all nine TPBs and to minimal overturning moment effects, showed the best agreement between measured response and target hysteresis.

3.2. Shake Table Tests versus Production Tests

Fig. 10 compares the response of Bearing SW from the production test, sinusoidal motion, and 88%-

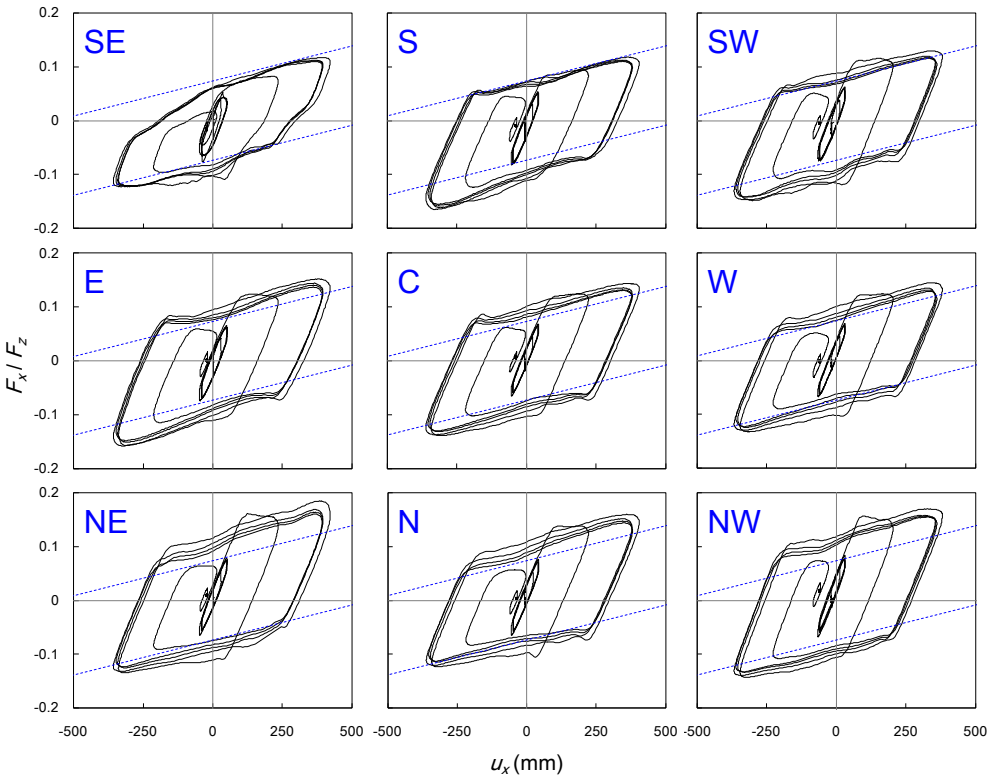

Figure 9. Hysteretic response obtained from sinusoidal test

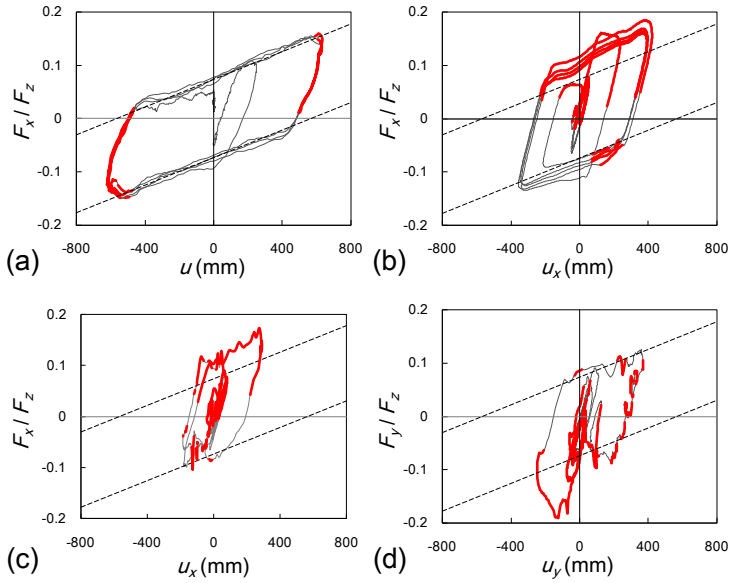

Figure 10. Hysteretic response from: (a) production test; (b) sinusoidal test; (c) X-response of 88%-XYZ Rinaldi motion; and (d) Y-response of 88%-XYZ Rinaldi motion.

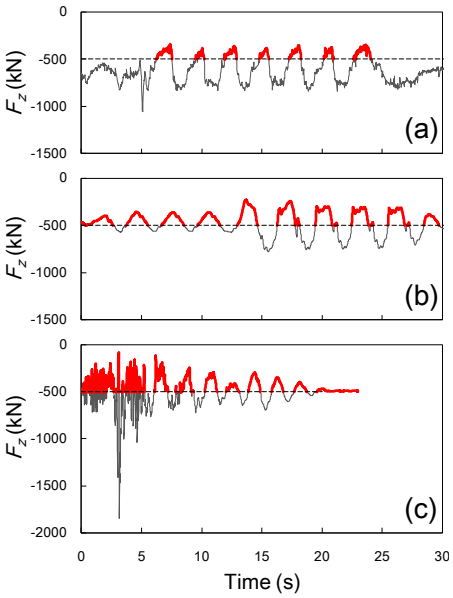

Figure 11. Compression from: (a) production test; (b) sinusoidal test; and (c) 88%-XYZ Rinaldi motion.

XYZ Rinaldi motion. For each of the three cases, Fig. 11 shows the time history of the compression acting in this bearing. In both figures, the duration when the compression is smaller than 500 kN is indicated by bold lines. The compression applied in the static state was 600 kN in the production tests and about 450 kN while on the shake table. During the production tests, the compression reduced with displacement, and reduced during the unloading part of the loading cycle (when stages 0 and 1 in Fig. 7 was activated). During the sinusoidal test, SW was subjected to compression in the range of 250 to 500 kN when the outer sliders were activated (stage 2) in positive F_x. During the 88%-XYZ Rinaldi motion, Bearing SW experienced substantial variation in compression due to overturning moment and vertical ground motion. In all cases, the friction coefficient for stage 2 was near 0.08 when the compression was greater than 500 kN but the friction coefficient increased beyond 0.08 when the compression was smaller than 500 kN. Mokha et al. (1990) and Takahashi et al. (2005) note that the friction coefficient in Teflon bearings tends to increase with pressure decrease if the pressure is below a threshold value. Figs. 9 and 11 suggest that the threshold compression beneath which the friction coefficient of the outer slider becomes dependent on pressure was near 500 kN for these particular TPBs. The normalized hysteresis from the production test and sinusoidal motion are very stable, while the normalized hysteresis from the 88%-XYZ Rinaldi motion is very irregular. The irregularity is mostly due to the small compression applied to this bearing during much of the test.

3.3. Response to Ground Motions

Based on a simple zero-cross counting method and wavelet analyses of the displacement history, the fundamental response period of the TPBs during the ground motion excitations was estimated as 2.0 to 2.2 seconds. This period is between the 1.84 seconds for stage 1 in Fig. 7 and 5.57 seconds for stage 2, but much closer to the former. As discussed by Sasaki et al. (2012), little torsional motion was measured in the TPB system despite the large mass eccentricity in the roof. While all nine bearings were subjected to very similar displacement histories, the reaction forces differed substantially.

Figs. 12 and 13 show the response of Bearing NE during the 100%-XY Iwanuma and 100%-XYZ Takatori motions, respectively. The Iwanuma motion is long ground motion record lasting nearly 5minutes. The 100%-XYZ Takatori motion produced the largest displacements in the TPBs among all 21 motions. In each figure, (a) and (b) show the hysteresis with the horizontal force F_x and F_y as the ordinate, while (c) and (d) take the normalized force F_x/F_z and F_y/F_z as the ordinate. Figures (a) and (b) indicate that Bearing NE developed larger resistance in positive F_x and negative F_y. The

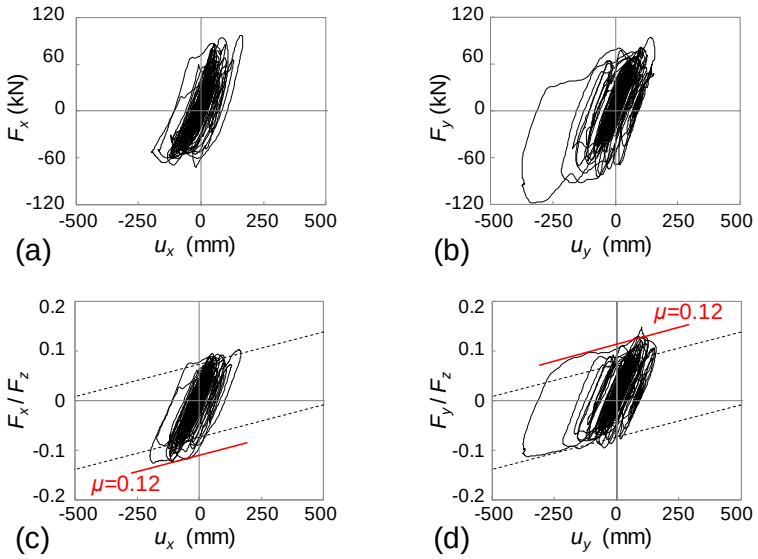

Figure 12. Response of Bearing NE during 100%-XY Iwanuma motion: (a) X-response; (b) Y-response; (c) normalized X-response; and (d) normalized Y-response.

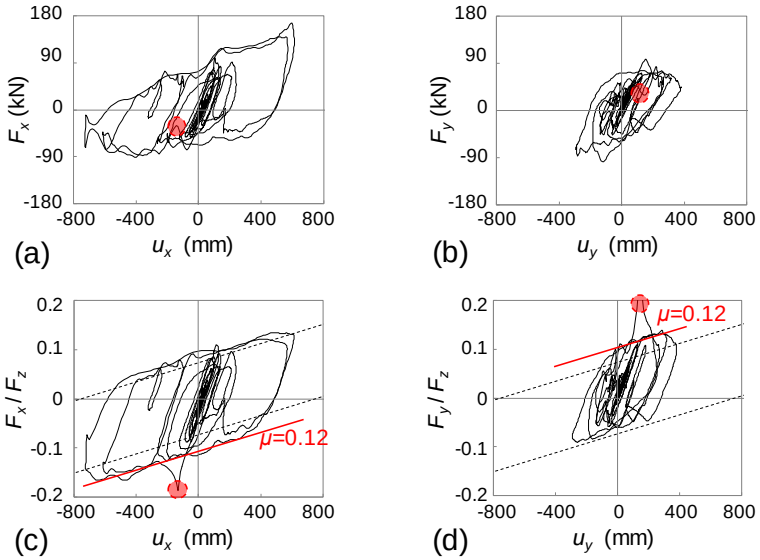

Figure 13. Response of Bearing NE during 100%-XYZ Takatori motion: (a) X-response; (b) Y-response; (c) normalized X-response; and (d) normalized Y-response.

non-symmetric hysteresis was caused by the overturning moment in the superstructure that varied the compression in the corner bearings. Figures (c) and (d) indicate that, as discussed in the previous section, the friction coefficient of the outer sliders exceeded the targeted 0.08 by 50% during the excursion of small compression. Fig. 13(c) and (d) show short spikes in the normalized reaction. The spikes corresponded to instances when the compression reduced to below 200 kN. While Fig. 13(a) and (b) show high-frequency oscillation in the reaction forces, the oscillation is less apparent in Fig. 13(c) and (d). Therefore, although the light weight of the superstructure and overturning moment in the superstructure caused many prolonged instances when the TPBs were subjected to compression smaller than 500 kN, the TPBs exhibited stable and reliable response that follow the target hysteresis.

3.4. Uplift

As mentioned earlier, the Rinaldi and Tabas motions have very severe UD components. The peak table acceleration was measured as 1.18g for the 88%-XYZ Rinaldi motion and 0.55g for the 80%-XYZ Tabas motion. During the 88%-XYZ Rinaldi motion, all bearings except SW experienced

uplift at some instant. During the 80%-XYZ Tabas motion, Bearings N, S, E, C, SE, and NW experienced uplift. Interestingly, uplift was observed frequently in the center bearing C, which is least affected by overturning moment, and not in the corner bearing SW, which was subjected to small gravity load and expected to be affected substantially by bidirectional overturning moments.

Figs. 14 and 15 shows the time history of the vertical shake-table acceleration and the compression in Bearings C and SW. Fig. 14 shows the history from the 88%-XY and 88%-XYZ Rinaldi motions, while Fig. 15 shows the history from the 100%-XY and 80%-XYZ Tabas motions. During both motions, Bearing C experienced short time durations when the measured vertical force was negligible. The TPBs were not provided with a mechanism to resist tension. Therefore, components of the TPBs disengaged, and allowed uplift, when the compression reduced to zero. On the other hand, Bearing SW did not experience any instance of zero vertical force. The figures also indicate that vertical motion excited high-frequency, vertical vibration modes of the superstructure that were not excited when the vertical motion was absent. The period of the vertical force response was 0.1 seconds or shorter, which is much shorter than the fundamental vibration period of the superstructure (0.7 seconds). While the 0.1 second period seems to roughly match the dominant period of the vertical shake-table acceleration, the occurrence of uplift did not synchronize with the instant of peak negative shake-table acceleration. The high-frequency fluctuation in compression was extremely large in Bearing C but not as large in Bearing SW. Bearing C uplifted for several prolonged durations of 0.1 to 0.3 seconds during the two XYZ motions. Study is ongoing to understand the vertical vibration of the superstructure and the mechanism that caused the observed uplifts.

3.5. Residual Displacements and Forces

Fig. 16 illustrates the residual X and Y displacements and forces at the end of major excitations. The selected cases left the largest residual displacements among the 21 motions. The largest residual displacement near 100 mm was measured after the 80%-XY Chichi motion (the 16-th out of the 21 motions) and the 100%-XY Tabas motion (9-th motion). Minimal residual torsions is noted in any of the four cases. The residual displacement did not accumulate over multiple motions. The largest residual force of 21 kN was measured at Bearing E after the 70%-XY Chichi motion (10-th motion). Considering that the gravity load at Bearing E was 800 kN, the residual force was nearly enough to activate the inner pendulum. The residual forces tended to form a torque in the counter-clockwise direction despite the absence of residual torsion. No appreciable change in displacements or forces was observed while the shake table was rested between excitations for one to eighteen hours.

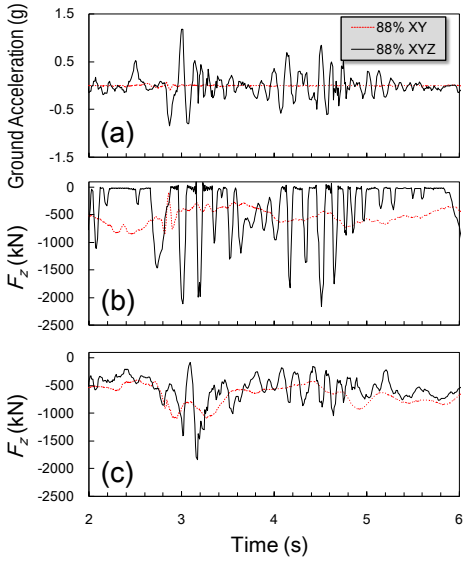

Figure 14. Time history from Rinaldi motions: (a) vertical table acceleration; (b) compression in bearing C; and (c) compression in Bearing SW.

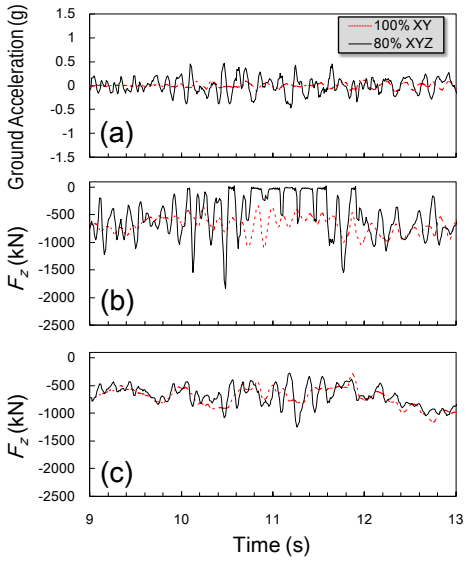

Figure 15. Time history from Tabas motions: (a) vertical table acceleration; (b) compression in bearing C; and (c) compression in Bearing SW.

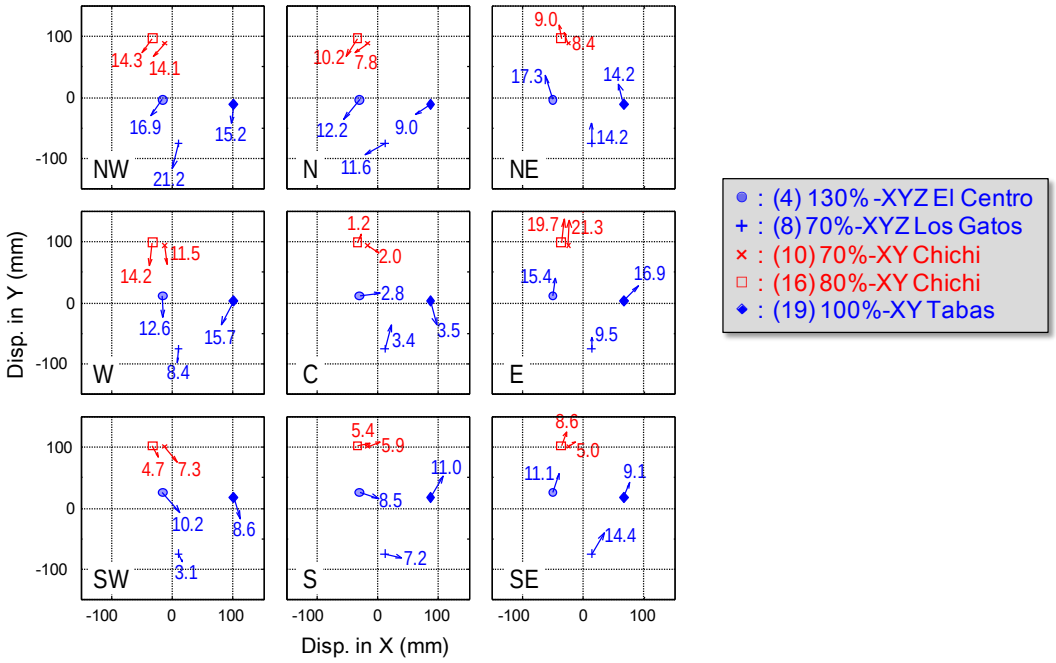

Figure 16. Residual displacements and forces (forces indicated in kN)

5. CONCLUSIONS

A full-scale, five-story, two bay-by-two bay, steel moment-frame building base isolated with triple-friction-pendulum bearings (TPBs) was subjected to a number of bidirectional (XY) and bidirectional-plus-vertical (XYZ) ground motions. A unique aspect of this shake-table test was that the three-directional force components were measured at all base-isolation devices. The aspect ratio of the building, taken as the height of mass center divided by the floor plan dimension, was 0.82 and 0.68 in the X and Y-directions, respectively. The overturning moment combined with the vertical shake-table motion produced substantial variation in the compression applied to the each bearing. Therefore, the test produced a rich set of data on full-scale TPBs subjected to a range of interesting dynamic loading conditions.

The response of the TPB system was affected by the light weight of the superstructure (very small static compression applied to TPBs), overturning moment in the superstructure, and vertical shake-table motion. The TPBs experienced many prolonged instances of small compression. The test results suggest that the friction coefficients of the outer pendulums increased by 50% when the compression applied on the TPBs reduced to below 500 kN. This is a relatively small compression for a base-isolation device. Vertical ground motion seemed to excite vertical vibration modes of the superstructure, and consequently, caused large variation in compression applied to the TPBs. In fact, the vertical motion was a greater cause of compression variation than overturning in the superstructure. Uplift was observed in eight of the nine TPBs during the 88%-XYZ Rinaldi motion. Although there were many prolonged instances when the TPBs were subjected to compression smaller than 500 kN, and most TPBs experienced uplift, the TPBs exhibited stable and reliable response that follow the target hysteresis. Overall, the TPBs provided excellent properties towards achieving horizontal base isolation. Effort is continuing to analyze the data obtained from the tests, and thereby, to further understand the performance of TPBs under realistic loading conditions.

ACKNOWLEDGEMENT

Funding for the research project was provided by the National Institute of Earth Science and Disaster Prevention of Japan and the U.S. National Science Foundation (Grants No. CMMI-1113275 and CMMI-0721399). The isolation devices and design service for the triple-pendulum bearings was donated by Earthquake Protection Systems. The views described in this paper are those of the authors and do not necessarily represent the

organizations mentioned herein.

REFERENCES

Fenz, D.M. and Constaninou, M.C. (2008). Spherical sliding isolation bearings with adaptive behavior: Theory. *Earthquake Engineering and Structural Dynamics* **37**,163-183.

Mokha A., Constantinou, M., and Reinhorn, A. (1990). Teflon bearings in base isolation. I: Testing. *Journal of Structural Engineering*, American Society of Civil Engineers, **116:2**, 438-454.

Morgan T.A. and Mahin S.A. (2011). The use of base isolation systems to achieve complex seismic performance objectives. *PEER Report 2011/06*, Pacific Earthquake Engineering Research Center, College of Engineering, University of California, Berkeley, Berkeley, California, U.S.A.

Ryan, K.L., Dao, N. D., Sato, E., Sasaki, T. and Okazaki, T. (2012). NEES/E-Defense base isolation tests: Interaction of lateral and vertical response. P*roceedings of the 15th World Conference on Earthquake Engineering*, Lisbon, Portugal, September 24-28, 2012.

Sasaki, T., Sato, E., Ryan, K.L., Okazaki, T., Mahin, S., and Kajiwara, K. (2012). NEES/E-Defense base-isolation tests: effectiveness of friction pendulum and lead-rubber bearings systems. *Proceedings of the 15th World Conference on Earthquake Engineering*, Lisbon, Portugal, September 24-28, 2012.

Soroushian, S., Ryan, K.L., Maragakis, M., Sasaki, T., Sato, E., Okazaki, T., Tedesco, L., Zaghi, A.E., Mosqueda, G., and Alvarez, D. (2012). NEES/E-Defense tests: Seismic performance of ceiling / sprinkler piping nonstructural systems in base isolated and fixed base building. P*roceedings of the 15th World Conference on Earthquake Engineering*, Lisbon, Portugal, September 24-28, 2012.

Takahashi, Y., Hibi, M., and Iemura, H. (2005). Numerical model for friction isolator considering multi-dependencies. *Journal of Applied Mechanics*, Japan Society of Civil Engineers, **8**, 701-708. (in Japanese).